



1 Carbonate content and stable isotopic composition of aerosol 2 carbon in the Canadian High Arctic

3

4 Petr Vodička^{1,2}, Kimitaka Kawamura², Bhagawati Kunwar^{2,3}, Lin Huang⁴, Dhananjay K.
5 Deshmukh^{2,a}, Md. Mozammel Haque^{2,5}, Sangeeta Sharma⁴, Leonard Barrie⁶

6

7 ¹ Institute of Chemical Process Fundamentals, Czech Academy of Sciences, 165 00 Prague 6, Czech Republic

8 ² Chubu Institute for Advanced Studies, Chubu University, 1200 Matsumoto-cho, Kasugai 487–8501, Japan

9 ³ Institute for Space-Earth Environmental Research, Nagoya University, Nagoya 464-8601, Japan

10 ⁴ Environment and Climate Change Canada, Science and Technology Branch, 4905 Dufferin St., Toronto, Canada

11 ⁵ School of Ecology and Applied Meteorology, NUIST, Nanjing, 210044, China

12 ⁶ Atmospheric and Oceanic Sciences Department, McGill University, Montreal, Canada

13 ^a Now at: Commission for Air Quality Management in National Capital Region and Adjoining Areas, New Delhi
14 110001, India

15

16 *Correspondence to:* Petr Vodička (vodicka@icpf.cas.cz) and Kimitaka Kawamura (kkawamura@isc.chubu.ac.jp)

17

18 **Abstract.** The carbon cycle in the Arctic atmosphere is important in understanding abrupt climate changes
19 occurring in this region. Two-years of measurements (summer 2016 - spring 2018) of carbonaceous
20 aerosols at the High Arctic station Alert, Canada, showed that in addition to organic carbon (OC) and
21 elemental carbon (EC), carbonate carbon (CC) was episodically but not negligibly present. The relative
22 abundances of CC in total carbon (TC) ranged from 0–65 % with an average of approximately 11 % over
23 the entire period. Also there was a strong correlation of CC with aerosol Ca²⁺ which is associated mostly
24 with soil dust and to a lesser extent sea salt aerosol. Based on this and the analysis of air mass back
25 trajectories (AMBT), we infer two possible sources of CC in the Arctic total suspended particles (TSP).
26 The major one is the erosion and resuspension of limestone sediments, particularly in the semi-desert areas
27 of the northern Canadian Arctic. Another potential more minor source of CC is from marine aerosol sources
28 including calcified marine phytoplankton shells (coccoliths) introduced into the atmosphere via sea-to air
29 emission.

30 The CC content significantly influenced the stable carbon isotopic composition ($\delta^{13}\text{C}$) of TC. The higher
31 the CC content, the higher the $\delta^{13}\text{C}$ values, which is consistent with the strong ^{13}C enrichment in carbonates.
32 Therefore, carbonates in Arctic TSP must be taken into account not only in isotopic studies using $\delta^{13}\text{C}$
33 analyses but also when assessing the impact of carbonaceous aerosols on the Arctic climate.



34

35 **1 Introduction**

36 The Arctic is a dynamically changing region that is significantly affected by climate change (England et al.,
37 2021). Aerosols are one of the factors influencing the climate, but their effects are subject to significant
38 uncertainties (Carslaw et al., 2013). The uncertainties in radiative forcing is primarily associated with
39 carbonaceous aerosols, most of which is composed of organic carbon (OC). In contrast, a smaller fraction
40 consists of elemental carbon (EC), which is equivalent to optically determined black carbon (BC) (Petzold
41 et al., 2013).

42 Organic aerosols, i.e., OC in the atmosphere, generally have a cooling effect on the climate (Stjern et al.,
43 2016) except for the part called brown carbon (Laskin et al., 2015). On the other hand, EC or BC has the
44 warming effect, both in the atmosphere (Liu et al., 2020) and on snow surface (Flanner et al., 2007)
45 especially important in the Arctic. In addition, EC and BC measurements are also used to determine the
46 mass absorption cross section (MAC), a fundamental input to radiative transfer models (Mbengue et al.,
47 2021). The MAC is season- and station- specific (Savadkoohi et al., 2024), making it one of the parameters
48 in affecting the influence of aerosols on climate. If either EC or BC is determined inaccurately, the MAC
49 factor will be subsequently biased as well (Chen et al., 2021). Therefore, detailed knowledge of the
50 composition of carbonaceous aerosol in the Arctic is crucial for improving our understanding of their
51 impacts on the climate changes in this region.

52 Recent atmospheric studies from Tajikistan (Chen et al., 2021) and Tibet (Hu et al., 2023) indicate a
53 significant contribution of carbonates in total suspended particles (TSP), which may have a significant
54 effect on the determination of OC and EC (or BC). Those areas are characterized as arid desert regions with
55 sparse vegetation, large amounts of unconsolidated sediments, and lack of soil moisture, where the wind
56 erosion plays an important role in the aeolian processes such as atmospheric transports and dust deposits.
57 Arctic regions are affected by long range transport of dust and also contributed locally (Groot Zwaafink et
58 al., 2016; Sharma et al., 2019; Sirois and Barrie, 1999). They have a desert, semi-desert or arid character in
59 some cases (Pushkareva et al., 2016). Recently high-latitude dust sources have been described as a
60 significant climate and environmental factor (Kawai et al., 2023; Kawamura et al., 1996; Meinander et al.,
61 2022). High Arctic semi-desert aerosols have been described as potentially important reservoirs of soil
62 organic matter (Muller et al., 2022), however, the influence of carbonates on the atmosphere in these regions
63 has not yet been systematically studied. Investigation of the ion balance of November to May fresh snowfall
64 at Arctic site Alert over a three year period (Toom-Sauntry and Barrie, 2002) led to the conclusion that
65 missing carbonate (especially in November and May) is the most likely cause of the ion imbalance.



66 In recent years, carbon in aerosols has also been subject to analyses of the stable isotopic composition ($\delta^{13}\text{C}$)
67 as a method for studying atmospheric processes (Gensch et al., 2014; Huang et al., 2006). Several studies
68 within the Arctic have also employed $\delta^{13}\text{C}$ analysis to study carbonaceous aerosols. Specifically, at the
69 Canadian Alert station, studies investigating $\delta^{13}\text{C}$ changes in the EC (Rodríguez et al., 2020; Winiger et al.,
70 2019) and springtime $\delta^{13}\text{C}$ changes in the TC (Narukawa et al., 2008) have recently been published.

71 Carbonates are strongly enriched in ^{13}C , with relatively positive $\delta^{13}\text{C}$ around zero, and can thus affect $\delta^{13}\text{C}$
72 values in TC of TSP aerosols, as demonstrated by Chen et al. (2016) for Asian desert dust. In the Arctic
73 region, observed higher aerosol $\delta^{13}\text{C}$ values are often attributed to dissolved particulate organic matter from
74 marine aerosol sources while the influence of carbonates are ignored (Gu et al., 2023). We hypothesized
75 that the influence of carbonates on Arctic aerosols is not negligible. In this study, we present two years of
76 carbonaceous aerosol observations at the Alert focusing on carbonate content and the isotopic composition
77 of $\delta^{13}\text{C}$ of TC.

78

79 **2 Experimental**

80 **2.1 Measurement site and sampling**

81 TSP samples were collected at the WMO Global Atmosphere Watch Observatory at Alert, Nunavut, Canada
82 ($82^{\circ}27'03.0''$ N, $62^{\circ}30'26.0''$ W, 210 m ASL). The Alert site represents a remote Arctic area located on the
83 northeastern tip of Ellesmere Island, which is 817 km from the North Pole (**Fig. 1**). The site has been used
84 for research on atmospheric aerosols since the mid-1980s (Barrie and Barrie, 1990). In terms of
85 carbonaceous aerosols, BC has been measured at the station for decades (Sharma et al., 2004, 2017).
86 Rodríguez et al. (2020) later then reported EC/OC results from TSP between March 2014 to June 2015 with
87 a focus on EC analyses.

88 For this study, TSP samples were collected from June 13, 2016 to April 16, 2018, using a high-volume
89 sampler on pre-baked (450°C , 12 h) quartz fiber filters (20 x 25 cm, PALL, 2500QAT-UP). During this
90 period, a total of 93 samples were collected at weekly intervals. The sampled filters were placed in clean
91 glass jars with Teflon-lined caps and stored in a freezer before chemical analyses.

92



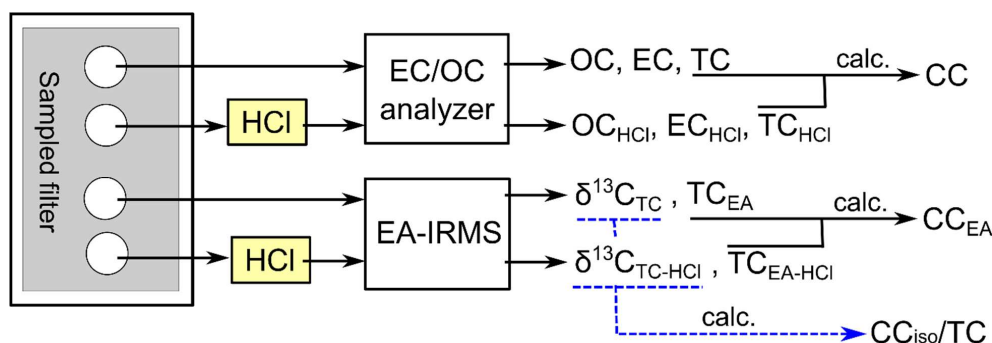
93

94 **Figure 1.** Map of the site position (asterisk) and geographical boundaries for dominant source regions of
95 backward air mass trajectories (Arctic Ocean - blue, Greenland - green, North Canada islands - red, North
96 America - purple, Siberia - grey, and Europe - yellow). Background map by Wikimedia Commons / Public
97 Domain.

98

99 2.2 Analyses

100 To obtain the TSP mass concentration, each filter was weighed before and after sampling, and resulting
101 concentrations were corrected for the corresponding field blank filter. Subsequently, we analyzed the
102 samples by two methods to measure the carbonaceous components, with the outputs shown in **Fig. 2.**



103

104 **Figure 2.** Diagram showing the method for the measurements of carbonaceous components in quartz fiber
105 filter samples.

106

107 Contents of OC, EC and total carbon (TC) were determined using a Sunset semi-continuous analyzer
108 (Sunset Laboratory Inc., Tigard, OR, USA; (Bauer et al., 2009)) operated in off-line mode. Samples with a
109 diameter of 16 mm (area 2.01 cm²) were analyzed by Improve_A temperature protocol: step [gas]
110 temperature (°C)/duration (s): helium (He) 140/120, He 280/120, He 480/120, He 580/120, He-O₂ (Ox.)
111 580/120, He-Ox. 740/120, He-Ox. 840/210 (Chow et al., 2007). Split point between OC and EC was
112 determined based on laser beam (660 nm) transmittance measurements through the filter during analysis
113 and raw data were subsequently evaluated by RTCalc726 software (Sunset Lab). The same EC/OC analysis
114 was performed after exposing the aerosol filters to HCl vapors overnight in a desiccator. From the difference
115 of TC and TC_{HCl}, the content of CC was calculated, which is discussed further in subsection 2.3.

116 The same samples were further analyzed for the stable carbon isotopic composition (δ¹³C) of TC by the
117 method described in more detail elsewhere (Vodička et al., 2022). Briefly, filter cuts (2.01 cm²) were placed
118 in tin cups, inserted into the elemental analyzer (EA, Flash 2000) and heated to 1000 °C in a helium
119 atmosphere. At this temperature, carbonaceous compounds are evolved and catalytically oxidized to CO₂,
120 which was isolated on a packed gas chromatograph, and then measured for TC by a thermal conductivity
121 detector, and finally transferred into the isotope ratio mass spectrometer (IRMS; Delta V, Thermo Fischer
122 Scientific) via a ConFlo IV interface for the analyses of ¹³C/¹²C ratios. An external standard, acetanilide
123 (supplied by Thermo Electron Corp.), having a δ¹³C of -27.26 ‰ compared to Vienna Pee Dee Belemnite
124 (VPDB), was used to obtain calibration curves for total carbon (TC) and its isotopic values. Subsequently,
125 we determined the δ¹³C of TC using Eq. (1) with relation to the international standard VPDB.

126
$$\delta^{13}\text{C} (\text{‰}) = [({}^{13}\text{C}/{}^{12}\text{C})_{\text{sample}} / ({}^{13}\text{C}/{}^{12}\text{C})_{\text{standard}} - 1] \times 10^3 \quad (1)$$



127 In this manner, $\delta^{13}\text{C}_{\text{TC}}$, corresponding to delta TC values on the filter, and $\delta^{13}\text{C}_{\text{TC-HCl}}$, representing delta
128 values on filters after exposure to HCl vapor, were analyzed. The standard deviation of $\delta^{13}\text{C}$ measurements
129 based on triplicate sample analysis was 0.03 ‰.

130 Through these analyses, we obtained TC from two independent analytical techniques. We observed good
131 agreement between TC value measured by the EC/OC analyzer and those by EA ($r = 0.99$). We also
132 obtained a good agreement even after HCl treatment of the filters ($r = 0.98$) (**Fig. S1**).

133

134 2.3 Characteristics of carbonate carbon (CC)

135 Concentrations of CC, one of the key variables of this study, were calculated from the difference of TC
136 before and after HCl fumigation (**Eq. (2)**)

$$137 \text{CC} = \text{TC} - \text{TC}_{\text{HCl}} \quad (2)$$

138 **Eq. (2)** defines CC, or nominal CC. **Fig. 3** shows thermograms from OC-EC analyses of a selected sample
139 without HCl treatment (purple curve) and after HCl treatment (green curve). As shown in **Fig. 3**, the largest
140 material loss can be seen at the temperature step EC2, but for other samples we observed the largest material
141 losses in the EC1 and OC4 regions as well. These are temperature steps during which we should expect the
142 release of carbonate carbon (CC) (Cavalli et al., 2010; Chow et al., 1993). On the other hand, removal of
143 carboxylic acids (e.g. acetic or oxalic acid) can be expected at temperature steps OC2 and OC3 (Hasegawa,
144 2022). We also analyzed several carbonate and oxalate salt standards as a control (**Fig. S2**). The thermogram
145 of the sample with a pronounced peak in the EC2 region (**Fig. 3**) was most similar to that of CaCO_3 (**Fig.**
146 **S2**). Hence, it can be assumed that the significant peaks, removed by HCl in the EC2 region of thermogram,
147 are carbonate in origin. Nevertheless, it cannot be excluded that some of the prominent CC peaks in the
148 OC4 region are also from oxalates. The nominal CC may contain other minor carbon components. Here,
149 however, it should also be noted that the reported values of oxalates in the Arctic (see, e.g., Feltracco et al.
150 (2021), Svalbard) are an order of magnitude lower than the CC values we analyzed.

151 It is worth noting here that if we did not analyze CC, it would be determined as either OC or EC based on
152 the thermogram and automatic determination of the split point (**Fig. 3**). For both EC and OC, we calculated
153 the percentage of mass removed by HCl fumes as CC using an **Eqs. (3)** and **(4)**.

$$154 \text{EC}_{\text{removed}} (\%) = (\text{EC} - \text{EC}_{\text{HCl}}) / \text{EC} * 100 \quad (3)$$

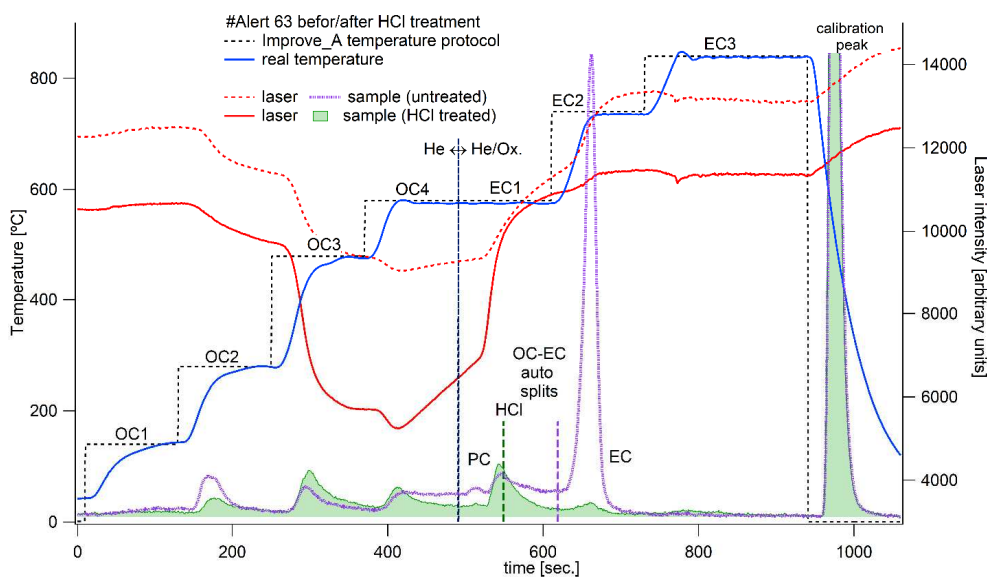
$$155 \text{OC}_{\text{removed}} (\%) = (\text{OC} - \text{OC}_{\text{HCl}}) / \text{OC} * 100 \quad (4)$$



156 In this way, we found that the CC contribution was, on average, 25 % (ranging from 0 to 81%) of EC and
 157 12 % (ranging from 0 to 46 %) of OC which have been inaccurately determined if we had not assessed the
 158 CC contribution. On a relative basis, EC concentrations were more biased in all seasons (**Fig. S3**).

159 Analyses for CC were performed by two independent methods (EC/OC and EA instruments, **Fig. 2**), and
 160 the resulting CC values show good agreement ($r = 0.87$, $y = 0.95 x$, **Fig. S4**). Unless otherwise stated, CC
 161 values calculated from EC/OC analyses are discussed in this study.

162



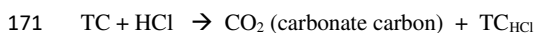
163

164 **Figure 3.** Example of EC/OC analysis of untreated (purple thermogram) and treated sample with HCl
 165 fumigation (green thermogram). Sample #Alert-63 was collected from 15-22 May 2017.

166

167 2.4 Estimate of $\delta^{13}\text{C}$ values of CC

168 The $\delta^{13}\text{C}$ analyses of TC and TC_{HCl} allowed us to estimate $\delta^{13}\text{C}$ of CC. Here we calculate the $\delta^{13}\text{C}$ values
 169 of released CC on HCl fumigation using the following reaction and the isotopic mass balance equation (**Eq.**
 170 **5**), being similar with the calculation in Kawamura and Watanabe (2004).





172
$$\delta^{13}\text{C}_{\text{TC}} = f * \delta^{13}\text{C}_{\text{CC}} + (1-f) * \delta^{13}\text{C}_{\text{TC-HCl}} \quad (5)$$

173 , where f means a fraction of CC in TC. From **Eq. 5**, we derived the formula for calculating $\delta^{13}\text{C}_{\text{CC}}$ (**Eq. 6**).

174
$$\delta^{13}\text{C}_{\text{CC}} = (\delta^{13}\text{C}_{\text{TC}} - (1-f) * \delta^{13}\text{C}_{\text{TC-HCl}}) / f \quad (6)$$

175 The $\delta^{13}\text{C}_{\text{CC}}$ values were reasonable for a CC content in the TC of approximately above 20 % (**Fig. S5**).
176 When f (CC contribution) is high, $\delta^{13}\text{C}_{\text{CC}}$ values are close to zero, supporting that CC is mainly composed
177 of carbonate, such as CaCO_3 . However, when the f values are low, the $\delta^{13}\text{C}_{\text{CC}}$ are highly scattered, indicating
178 that the released (removed) carbon by HCl is not only carbonate carbon but also contains various types of
179 carbon including semi-volatile organic acids or unknown species. In the case of organic acids, $\delta^{13}\text{C}$ values
180 can be as high as -10‰ (e.g., Wang and Kawamura, 2006) or positive due to unknown isotope fractionation
181 during analytical processing. Highly scattered values may also be due to potential analytical errors in EA-
182 IRMS measurements when f is sufficiently small. If the CC contribution were zero, **Eq. 6** would lead to
183 division by zero. This may also be the cause of bias and scattering of $\delta^{13}\text{C}_{\text{CC}}$ values at low CC contributions
184 (**Fig. S5**).

185

186 2.5 Carbonate estimation from isotopic composition

187 We used the isotopic mass balance between $\delta^{13}\text{C}_{\text{TC}}$ and $\delta^{13}\text{C}_{\text{TC-HCl}}$ as an alternative and probably more
188 accurate method to determine carbonate content (CC_{iso}) in TC. The $\text{CC}_{\text{iso}}/\text{TC}$ (f_{iso}) calculation is based on
189 the assumption that the $\delta^{13}\text{C}$ of carbonates is around 0‰ with an approximate range $+5\text{‰}$ to -5‰ , and no
190 other compounds are present in this range. We used **Eq. 5**, where $\delta^{13}\text{C}_{\text{TC}}$ and $\delta^{13}\text{C}_{\text{TC-HCl}}$ are known and $\delta^{13}\text{C}_{\text{CC}}$
191 are given by three different values, covering an approximate range of carbonates ($+5\text{‰}$, 0‰ , -5‰).

192 While $\delta^{13}\text{C}_{\text{CC}} = 0$, $f = 1 - (\delta^{13}\text{C}_{\text{TC}} / \delta^{13}\text{C}_{\text{TC-HCl}}) \quad (7)$

193 While $\delta^{13}\text{C}_{\text{CC}} = +5$, or -5 , $f = (\delta^{13}\text{C}_{\text{TC}} - \delta^{13}\text{C}_{\text{TC-HCl}}) / (\delta^{13}\text{C}_{\text{CC}} - \delta^{13}\text{C}_{\text{TC-HCl}}) \quad (8)$

194 The f_{iso} value is then an average calculated from the three f values obtained from **Eqs. 7** and **8**.

195

196 2.6 Auxiliary data

197 Air mass back trajectories (AMBT) were calculated using the National Oceanic and Atmospheric
198 Administration (NOAA) HYSPLIT model (Stein et al., 2015) at 500 m a.g.l. using a run time 168 h in
199 GDAS (Global Data Assimilation System) with 0.5 degree resolution for each sampling days. For
200 subsequent analyses, we divided the air masses into six sectors as depicted in **Fig 1**.



201 Meteorological data at 5 min resolution for temperature (T), wind speed (WS) and wind direction (WD)
202 were provided by Environment and Climate Change Canada. Only WDs between 14 November 2016 and
203 16 January 2017 were obtained from the NOAA website (<https://psl.noaa.gov/arctic/observatories/alert/>).
204 For the purpose of this study, complementary mean values of T and WS were calculated to each sample.

205 The WD and WS data were used to create wind roses by Zefir software (Petit et al., 2017) and used in
206 combination with the AMBT data to determine the predominant aerosol origin for each sample. All wind
207 roses and AMBT by HYSPLIT are shown in supplementary data.

208 The water soluble ions (Ca^{2+} , Mg^{2+} , Na^+) were measured using an ion chromatography (761 Compact IC,
209 Metrohm, Switzerland). For this purpose, the filtered samples were twice extracted with 10 ml of ultrapure
210 water using an ultrasonic bath for 15 min and the aqueous extracts were filtered using a disc filter (Millex-
211 GV, 0.22 μm , Millipore).

212

213 **3 Results and discussion**

214 **3.1 Carbonaceous aerosol composition**

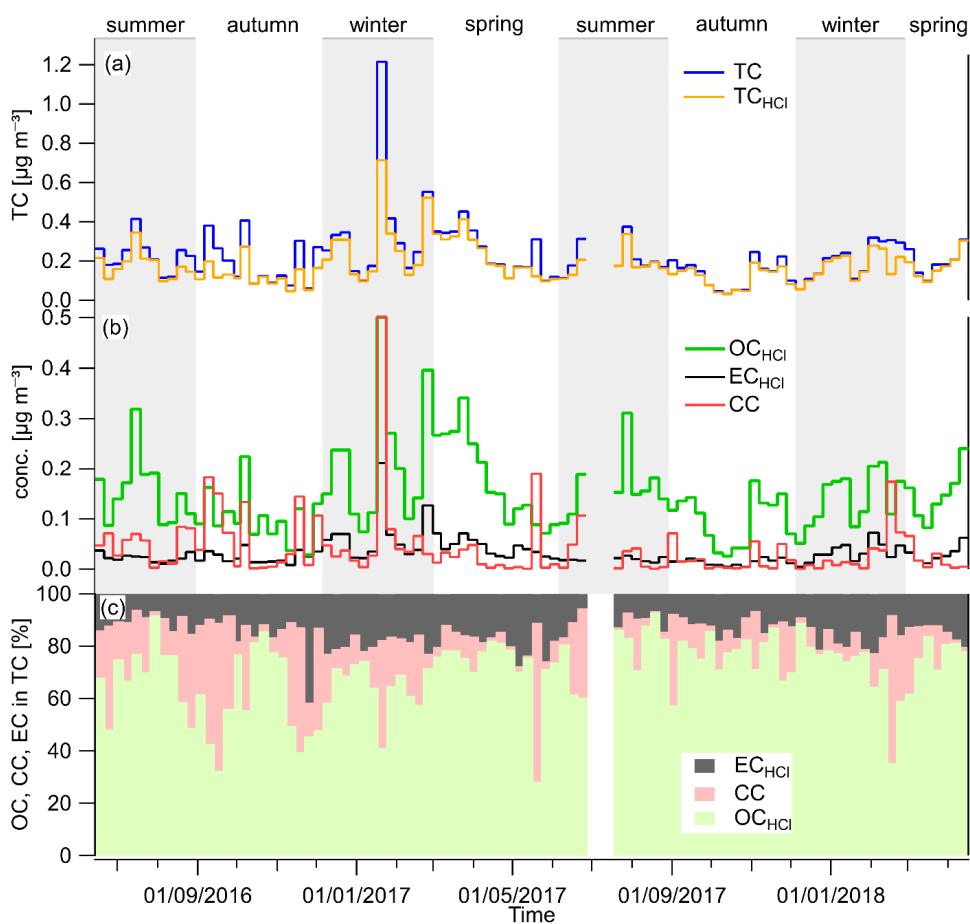
215 Time series of TC, OC_{HCl} , EC_{HCl} and CC mass concentrations are shown in **Fig. 4**. An overview of results
216 is provided for the seasonal variations from 2016 to 2018 in **Table 1** and **Fig. S6** in supplementary material.
217 An average TC concentration over the entire measurement period was $0.219 \pm 0.147 \mu\text{g m}^{-3}$ (median 0.186
218 $\mu\text{g m}^{-3}$; deviation due to one sample with a concentration of $1.22 \mu\text{g m}^{-3}$, **Fig. 4a**). Average TC contribution
219 in aerosol mass ranged from 5 to 14% (**Table 1**). Seasonally, the highest mass concentrations of TC, OC_{HCl}
220 and EC_{HCl} were found in winter and/or spring (**Fig. S6, Table 1**).

221 The fact that EC_{HCl} corresponds to realistic elemental carbon concentrations is demonstrated by comparison
222 with the study of Rodríguez et al. (2020), who analyzed EC in TSP during 2014-2015. They reported
223 seasonal EC concentrations that are similar to our observed EC_{HCl} , while their CC was part of the OC due
224 to the use of a different temperature protocol (EnCan-Total-900) during the OC/EC analysis. However,
225 Rodríguez et al. (2020) did not quantify the contribution of CC to TC.

226 Concentrations of OC_{HCl} dominate in all seasons (**Figs. 4b** and **5**) but present seasonally different
227 correlations with ambient temperature. Especially in summer, we observe a significant positive correlation
228 ($r = 0.73$) between OC_{HCl} concentrations and temperature (**Fig. S7a**). A similar relationship was also
229 observed, e.g., at the subarctic station Pallas (Friman et al., 2023), suggesting a biogenic origin of
230 summertime organic aerosols in Arctic areas (Moschos et al., 2022). In contrast, we observe negative
231 correlations between OC_{HCl} and ambient temperature in winter ($r = -0.15$, insignificant) and spring ($r = -$



232 0.43). A year-round similar trend for EC_{HCl} ($r = -0.39$, **Fig. S7b**), supporting previous studies that highlight,
 233 in particular, the anthropogenic contributions to Arctic aerosol during the polar night (Moschos et al., 2022).
 234 However, for CC, we observe no significant dependence on temperature ($r = 0.09$, **Fig. S7c**).
 235



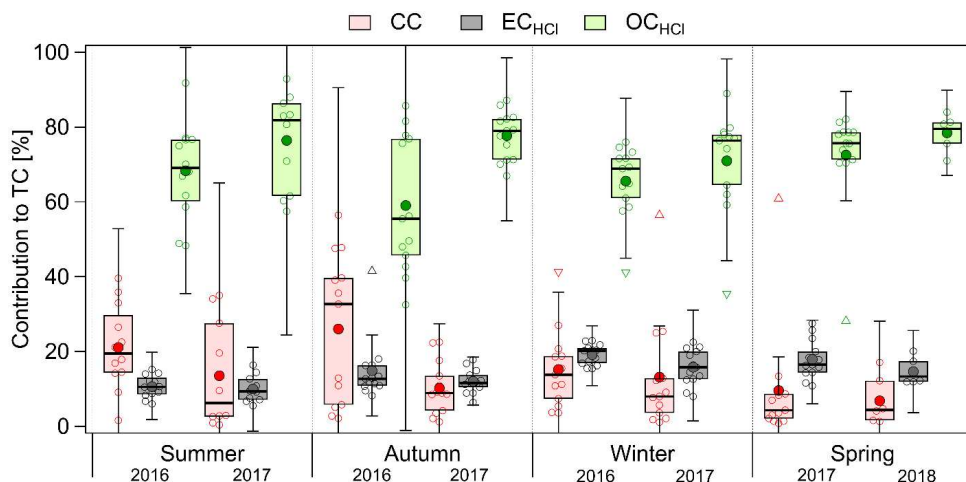
236
 237 **Figure 4.** Time series of (a) TC mass concentrations before and after HCl treatment of samples, (b) OC,
 238 EC and CC mass concentrations, and (c) their relative contributions to TC in the Alert TSP aerosols.

239
 240 Time series of TC before and after HCl fumigation (**Fig. 4a**) show that the amount of carbon removed in
 241 the form of CC is neither negligible nor large. However, both mass concentrations of CC (**Fig. 4b**) and its



242 relative contributions (**Fig. 4c**) show that the CC is often larger than the EC_{HCl} contribution. Specifically,
 243 CC concentrations were highest during both autumn of 2016 and summer of 2016 and 2017 (**Fig. S6c**),
 244 which was reflected also in the relative contributions to TC (**Table1, Fig. 5**).

245 It is notable to understand the origin of CC. During summer, the contribution of biogenic aerosols (a
 246 potential source of oxalates) is highest, while the landscape is least covered by snow, making the situation
 247 favorable for resuspension of soils eroded from rocks including carbonates. A potential source of carbonates
 248 may come directly from the Canadian Arctic land region, where limestone sediments are reported to be
 249 abundantly present (Groot Zwaaftink et al., 2016; Not and Hillaire-Marcel, 2012; Phillips and Grantz, 2001).
 250 Another likely source of carbonate is marine aerosols as marine organisms contribute carbonate to the sea
 251 (Stein et al., 1994). In the context of wind directions and the effect on $\delta^{13}\text{C}$, the origin of CC is further
 252 discussed in the following subsection 3.2.



253 **Figure 5.** Seasonal contributions of CC, EC_{HCl} and OC_{HCl} to TC. The boxes correspond to the interquartile
 254 range (IQR; 25 and 75 percentile) with median represented by the inner solid line. The whiskers correspond
 255 to inner fences range (1.5*IQR), triangles are outliers and mean is represented by large filled circle.
 256

257

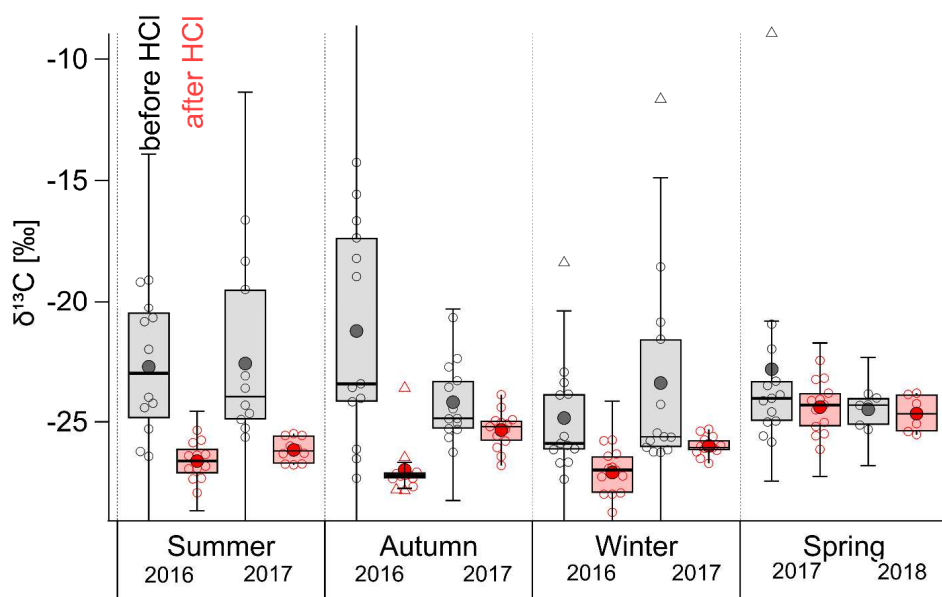
258 3.2. Stable carbon isotopic composition

259 Removal of CC by HCl fumigation has a significant effect on the measurements of $\delta^{13}\text{C}$ isotopic values of
 260 TC (**Figs. 6 and 7**). **Fig. 6** shows a seasonally resolved $\delta^{13}\text{C}$ values for HCl-treated (red) and untreated
 261 (grey) samples. We observed significant changes in all seasons except in spring of 2017 and 2018. Here it



262 is interesting to mention a link with Narukawa et al. (2008), who reported changes in $\delta^{13}\text{C}$ of TC values for
 263 HCl-treated samples between winter and spring at Alert site. Narukawa et al. (2008) show significantly
 264 higher $\delta^{13}\text{C}$ values in spring than winter and related this to the possible contribution of carboxylic acids
 265 (especially oxalic acid). During our observations, the differences in average values of $\delta^{13}\text{C}$ of TC (HCl
 266 treated vs. untreated) were also significant (see red boxes in **Fig. 6** and **Table 1**). Winter and spring $\delta^{13}\text{C}$
 267 values after HCl treatment in this study (**Table 1**) are similar to those presented by Narukawa et al. (2008)
 268 for the year 2000. Thus, this study confirms that this is a long-term phenomenon likely to occur annually.

269



270

271 **Figure 6.** Seasonal variations of $\delta^{13}\text{C}$ of TC of untreated (grey) and HCl treated (red) TSP samples at Alert
 272 site from summer 2016 to spring 2018. The boxes correspond to the interquartile range (IQR; 25 and 75
 273 percentile) with median represented by the inner solid line. The whiskers correspond to inner fences range
 274 ($1.5 \cdot \text{IQR}$), triangles are outliers and mean is represented by large filled circle.

275

276 In addition, measurements of $\delta^{13}\text{C}$ in OC, pyrolytic carbon (POC) + CC, and EC, performed at Environment
 277 Canada Toronto Laboratory, using ECT9 temperature protocol (Huang et al., 2006, 2021) for the fine
 278 particle (PM_{10}) samples collected around 2003, support that a noticeable fraction of CC occurs during the

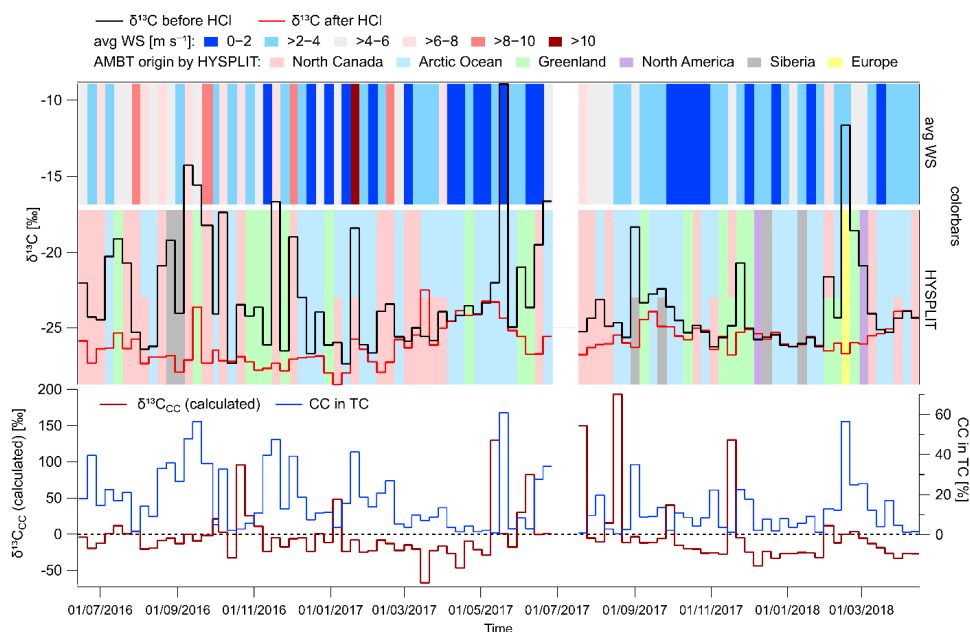


279 summer months, as indicated by the relatively more positive $\delta^{13}\text{C}$ of “POC+CC” fraction (**Fig. S8**).
280 Carbonate from eroded rocks in terrestrial environment usually generates large particulates, so the CC
281 content in PM_{10} should be lower than that in TSP. Consequently, the $\delta^{13}\text{C}$ TC in PM_{10} is expected to be
282 relatively less positive of compared to that that in TSP. Therefore, **Fig. S8** suggests that the impact of CC
283 on $\delta^{13}\text{C}$ TC is an annual phenomenon occurring over decadal periods. The tendency towards relatively more
284 positive $\delta^{13}\text{C}$ in summer OC fraction also suggests the presence of minor salt oxalate, or potassium or
285 magnesium carbonates, which are released at 550 °C or lower, as shown in **Fig. S2**. In the time series in
286 **Fig. 7**, we observed episodes with significant differences in $\delta^{13}\text{C}$ values and alternating over short periods.
287 The comparison of $\delta^{13}\text{C}$ of TC and TC mass concentration for both HCl untreated and treated samples
288 shows insignificant correlation (**Fig. S9**). However, we found a significant, though not strong, correlation
289 of $\delta^{13}\text{C}$ with wind speed (**Fig. S10**) ($r = 0.36$) and a negative correlation after HCl fumigation ($r = -0.32$ for
290 $\delta^{13}\text{C}_{\text{TC-HCl}}$ vs. wind speed). Concentrations of CC were also positively correlated with wind speed ($r = 0.48$,
291 **Fig. S10**), indicating that wind has an effect on this aerosol component. Therefore, we compared the $\delta^{13}\text{C}$
292 time series with average wind speeds and prevailing AMBTs from the HYSPLIT model (see colored bars
293 in **Fig. 7**), which were divided into six regions as shown in **Fig. 1**.

294 The large differences in $\delta^{13}\text{C}$ values (or relatively more positive $\delta^{13}\text{C}_{\text{TC}}$ values) can be divided into three
295 categories. The most frequent differences were observed during periods of stronger winds (average WS
296 above 4 m s^{-1}) associated with the prevailing back trajectories from the North Canada region. These episodes
297 can be found mainly in summer and autumn 2016 and summer 2017. Such conditions favor dust
298 resuspension, which may also contain limestone, known to be abundant in this region (Not and Hillaire-
299 Marcel, 2012; Phillips and Grantz, 2001). The presence of a peak in soil dust carbonates in late
300 summer/early autumn is consistent with multidecadal aerosol aluminum observations at Alert (Sharma et
301 al., 2019; Sirois and Barrie, 1999). These observations also indicate a peak in soil dust aerosol in the spring
302 month of May (Sharma et al. 2019).

303 Second, in late February/March 2018, we observed significant enrichment of ^{13}C , which may probably be
304 linked to long range transport (LRT) from/over Europe, Greenland and North America (Fig. 6). Sources of
305 carbonate in this case may be, for example, calcifying marine phytoplankton (Monteiro et al., 2016), which
306 are abundant in the North Atlantic (Okada and Honjo, 1973). Another possibility is the volcanic and
307 subarctic semi-desert areas in Iceland (Arnalds et al., 2016).

308



309

310 **Figure 7.** Time series of isotopic composition ($\delta^{13}C$) of TC before and after HCl treatment of samples
 311 (upper part) with color bars representing average wind speed (top) and origin of AMBT based on HYSPLIT
 312 model and divided to regions shown in Fig. 1 (middle part). Time series of the calculated $\delta^{13}C_{CC}$ together
 313 with contribution of CC in TC (bottom).

314

315 The third case is a $\delta^{13}C$ difference observed during lower wind speeds coming from the Arctic Ocean or
 316 Greenland. This includes also the sample taken between 15-22 May 2017, whose thermograms are shown
 317 in **Fig. 3**, and which was most enriched in ^{13}C carbon. A recent study by Gu et al. (2023), which reports
 318 observations of summer carbonaceous aerosols in the Arctic Ocean, is relevant in this context. They also
 319 observed relatively more negative $\delta^{13}C$ values of TC, but in this case they did not consider the enriched ^{13}C
 320 carbon as a carbonate contribution, instead, they associated it with an input of fresh marine particulate
 321 organic carbon (MPOC) (Verwega et al., 2021). MPOC is formed by the conversion of inorganic carbon
 322 by marine phytoplankton through photosynthesis in ocean surface layer (Descolas-Gros and Fontugne,
 323 1990), and this carbon can be partially released into the atmosphere as marine aerosol (Ceburnis et al.,
 324 2016). We cannot exclude the influence of MPOC on the TSP taken at the Alert station, but the specific
 325 EC/OC thermogram (**Fig. 3, Fig. S2**) shows rather an influence of $CaCO_3$. The presence of carbonates in
 326 surface seawater and their interference with organic coatings has been known for decades (Chave, 1965).

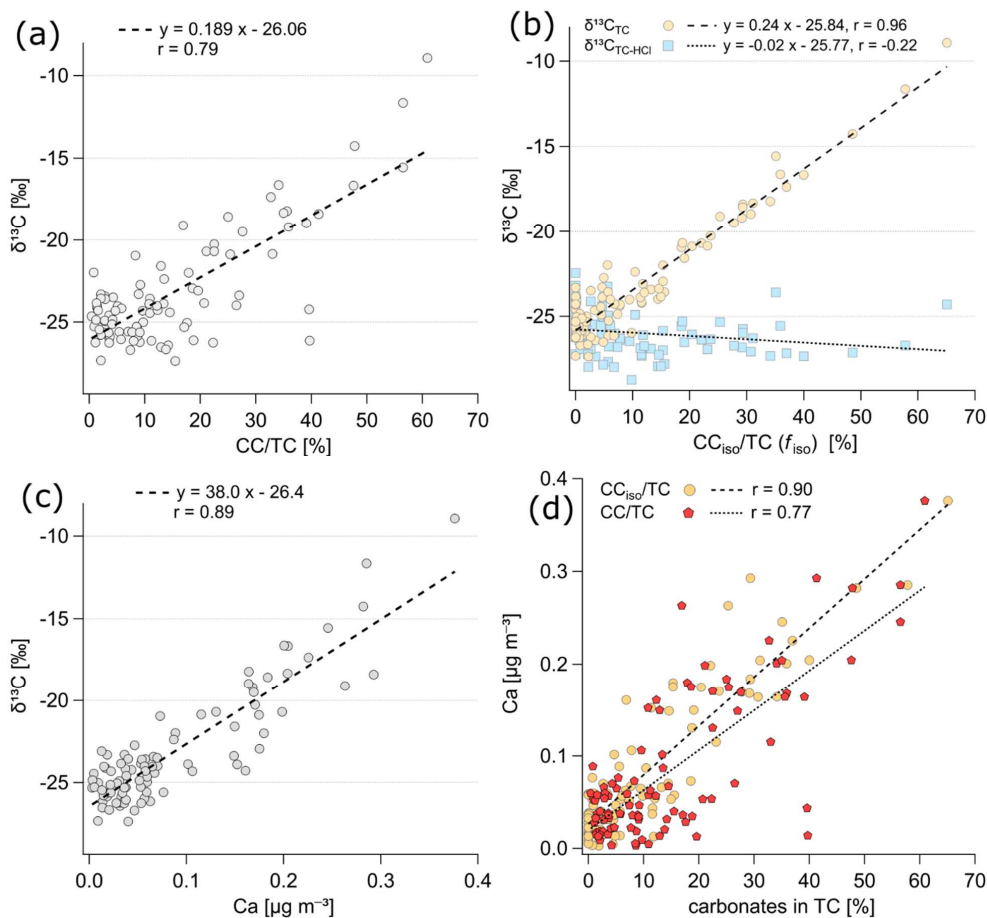


327 Dissolved CO₂ in the oceans consists mainly of inorganic substances, which are bicarbonates (HCO₃⁻;
328 >85%) and carbonates (ca 10%), and their content varies with temperature, pH, salinity and other
329 parameters (Zeebe, 2012). Carbonate, in the form of CaCO₃, is generally supersaturated in surface seawater
330 but its precipitation may be limited due to dissolved organic matter (Chave and Suess, 1970). In addition
331 to common inorganic reactions due to dissolved CO₂, the carbonate cycle is also influenced by marine life.
332 Phytoplankton such as coccolithophores (e.g. *Emiliana huxleyi*), could also contribute to formation of
333 carbonates (Smith et al., 2012). These organisms produce calcified shells called coccoliths, which are about
334 2–25 µm across (Monteiro et al., 2016). While these microfossils are mostly deposited on the seabed, they
335 are also likely to be released also into the atmosphere with marine aerosol from the upper sea layers.
336 Whether through MPOC or inorganic carbon, this phytoplankton influences the fractionation of ¹³C carbon
337 (Holtz et al., 2017).

338 Coccolith microfossils contain enriched calcite with δ¹³C values around 0 ‰ (McClelland et al., 2017).
339 Limestone sediments in the Canadian Arctic are even more enriched, with δ¹³C values ranging from 2 to
340 8 ‰ (Beauchamp et al., 1987). After estimating δ¹³C_{CC} (see subsection 2.4), we observed that with a high
341 CC abundance in TC, the calculated δ¹³C_{CC} values are also seen around 0 ‰ (**Fig. 7** bottom, **Fig. S5**). This
342 suggests that when the TC contains a larger contribution of CC (suppose above 20%), it can be assumed
343 that a significant portion of the nominal CC is derived from limestone. However, the uncertainties in the
344 determining of δ¹³C_{CC}, mentioned in section 2.4, primarily due to the low CC contributions in TC, likely
345 prevent distinguishing whether the carbonates are from sediment resuspension or marine calcified shells.
346 Some insight, however, can be obtained from the AMBT analysis discussed earlier.

347 Finally, **Fig. 8a** confirms a strong dependence of δ¹³C_{TC} on the CC content in TC (r = 0.79). The dependence
348 of δ¹³C_{TC} directly on CC mass concentration is even stronger (r = 0.85, after excluding 1 outlier, **Fig. S11**).
349 Furthermore, we calculated the fractions of CC for individual samples via isotope mass balance (using a
350 δ¹³C of CC value of zero as the end member, see subsection 2.5.) and found that, overall, the calculated
351 results were approximately 5 % lower than the measured CC/TC, with less scatter. In addition, we observed
352 an excellent correlation between δ¹³C of TC and the calculated fraction of CC, with r = 0.96 shown in **Fig.**
353 **8b**, indicating that more than 92 % of the variation in δ¹³C of TC can be explained by the dependency on
354 the fraction of CC.

355



356

357 **Figure 8.** Dependence of (a) $\delta^{13}\text{C}_{\text{TC}}$ on the percentage contribution of CC in TC, (b) $\delta^{13}\text{C}_{\text{TC}}$ and $\delta^{13}\text{C}_{\text{TC-HCl}}$
 358 on the calculated fraction of CC_{iso} in TC, (c) $\delta^{13}\text{C}_{\text{TC}}$ on Ca mass concentrations, and (d) Ca mass
 359 concentrations on percentage contribution of CC and CC_{iso} in TC.

360

361 Further support for the influence of $\delta^{13}\text{C}$ of TC in favor of carbonates is provided by its strong correlation
 362 with calcium ($r = 0.89$, **Fig. 8c**). Calcium is also strongly correlated with CC contribution in TC, with $r =$
 363 0.90 for Ca vs. $\text{CC}_{\text{iso}}/\text{TC}$ (**Fig. 8d**). Apportionment of Ca amongst aerosol sources at Alert site (Sharma et
 364 al., 2019), using multidecadal observations and Positive Matrix Factorization analyses, showed that, on



365 average for both the period November to February, and March to May, Ca was associated 84 and 85% with
366 windblown dust/soil and 12 and 8 % with sea salt aerosol, respectively.

367 We also investigated the possible contribution of carbon from magnesium carbonate. Magnesium was
368 strongly correlated with sodium ($r = 0.91$, **Fig. S12**), indicating its link mainly to marine aerosol. In contrast,
369 we observed no relationship between Mg and Ca; this dependence was strongly scattered (**Fig. S12**). Overall,
370 the results indicate that the main contribution of CC, that strongly influences the $\delta^{13}\text{C}$ of TC, is mainly
371 CaCO_3 . If there is a contribution of magnesium carbonate, it is rather episodic.

372 These results thus provide evidence that the CC content in aerosols, mostly of soil origin and to a lesser
373 extent marine origin, strongly influences the $\delta^{13}\text{C}$ isotopic composition of TC in the Arctic atmosphere.
374 Further research at different Arctic sites could reveal whether the non-negligible presence of CC in the TSP
375 is the case only in the northern Canada region or a phenomenon observe in larger parts of Arctic.

376

377 **4 Summary and conclusions**

378 We found that the aerosol CC (i.e. carbonate carbon) fraction in Arctic TSP at Alert site is not negligible.
379 The relative abundances of CC in TC ranged from 0 to 60 % with an average of 11 % over the entire
380 measurement period. On average, 25 % (range: 0 to 81 %) of EC and 12% (range: 0 to 46 %) of OC was
381 identified here as nominal CC. The influence of CC removal from the sample was also significantly
382 reflected in the isotopic composition of $\delta^{13}\text{C}$ of TC. The effect of CC on $\delta^{13}\text{C}$ was particularly pronounced
383 in the summer of 2016 and 2017, as well as during autumn 2016 due to strong local Arctic dust transport.
384 In contrast, the effect of removing of CC on $\delta^{13}\text{C}$ was lowest in spring. Thus, CC content in TSP at Alert
385 can sometimes strongly influence the $\delta^{13}\text{C}$ values of aerosols.

386

387 Based on the thermograms from EC/OC analyses and the calculated $\delta^{13}\text{C}_{\text{CC}}$, whose values were around 0‰
388 at high CC contributions to TC, we conclude that the major part of CC is derived from carbonates.
389 Additionally, based on the isotope mass balance calculation (using 0‰ as $\delta^{13}\text{C}_{\text{CC}}$), an excellent dependency
390 between $\delta^{13}\text{C}$ of TC and the calculated fraction of CC ($r = 0.96$) is observed, supporting that most of the
391 variation of $\delta^{13}\text{C}$ of TC were due to the contribution of CC. Based on the AMBT analyses, we identified
392 two possible carbonate sources. The first is eroded and resuspended limestone sediments in the northern
393 Canadian region. The second source may be calcareous shells (coccoliths) produced by marine
394 phytoplankton and transported from both the Arctic Ocean and the North Atlantic Ocean. However, the
395 hypothesis of these sources requires further detailed research.

396



397 In general, when analysing $\delta^{13}\text{C}$ of TC in coarse aerosol or aerosols laden with dust, it must be taken into
398 account that the resulting values may be strongly influenced by CC content. If CC is not removed prior to
399 EC/OC analysis, CC may be mistakenly identified as EC during Improve_A analysis. This could, for
400 example, affect modelling of the effect of carbonaceous aerosols on the Arctic climate, as EC (or black
401 carbon) has a warming effect on the atmosphere, while CC likely has the opposite effect.

402

403 **Data availability.** All relevant data for this paper are archived and are available upon request from the
404 corresponding authors or online at repository here: <https://zenodo.org/records/14204515>

405

406 **Supplementary data**

407 Supplementary data to this article can be found as a pdf file uploaded together with this manuscript.

408

409 **Author contribution.** All authors contributed to the final version of this article. PV analyzed EC/OC
410 before and after HCl treatment, as well as $\delta^{13}\text{C}$ of TC, AMBT analyses, evaluated all data and wrote the
411 paper under the supervision of KK. BK analyzed $\delta^{13}\text{C}$ of TC after HCl treatment as well as supporting water
412 soluble ions measurements. LH calculated contribution of $\text{CC}_{\text{iso}}/\text{TC}$ based on $\delta^{13}\text{C}$ measurements. DD and
413 MMH assisted in the gravimetry and other sample treatments. SS provided meteorological data. SS with
414 KK and LB managed the field campaign. All authors provided advice and feedback throughout the drafting
415 and submission process.

416

417 **Competing interests.** Kimitaka Kawamura is an editor for Atmospheric Chemistry and Physics. The
418 authors declare that they have no other conflict of interest.

419

420 **Acknowledgements.** This study was supported by JSPS grant no. 24221001, the JSPS Joint Research Program
421 implemented in association with DFG (JRP-LEAD with DFG: JPJSJRP 20181601) and from the Ministry of
422 Education, Youth and Sports of the Czech Republic under project ACTRIS-CZ LM2023030. Authors thank the CFS
423 Alert for maintaining the base, Andrew Platt Alert coordinator, the operator for ECCC and students for sample
424 collection at Alert and shipment of these samples.

425

426



427

428 **Table 1:** Seasonal averages \pm standard deviations (medians in parentheses) of different variables in TSP at
429 Alert site.

	Summer 2016	Autumn 2016	Winter 2016	Spring 2017	Summer 2017	Autumn 2017	Winter 2017	Spring 2018
N	12	13	13	13	10	13	13	6
OC [$\mu\text{g m}^{-3}$]	0.182 \pm 0.0 75 (0.177)	0.136 \pm 0.0 72 (0.106)	0.253 \pm 0.1 71 (0.237)	0.184 \pm 0.0 92 (0.151)	0.179 \pm 0.0 71 (0.155)	0.106 \pm 0.0 6 (0.128)	0.154 \pm 0.0 57 (0.177)	0.154 \pm 0.0 53 (0.153)
EC [$\mu\text{g m}^{-3}$]	0.037 \pm 0.0 21 (0.032)	0.056 \pm 0.0 55 (0.023)	0.100 \pm 0.1 21 (0.070)	0.057 \pm 0.0 37 (0.047)	0.031 \pm 0.0 15 (0.026)	0.019 \pm 0.0 13 (0.017)	0.055 \pm 0.0 36 (0.046)	0.032 \pm 0.0 18 (0.029)
TC [$\mu\text{g m}^{-3}$]	0.219 \pm 0.0 82 (0.216)	0.193 \pm 0.1 20 (0.126)	0.353 \pm 0.2 87 (0.290)	0.240 \pm 0.1 13 (0.186)	0.210 \pm 0.0 76 (0.186)	0.125 \pm 0.0 70 (0.146)	0.209 \pm 0.0 88 (0.225)	0.186 \pm 0.0 71 (0.182)
OC _{HCl} [$\mu\text{g m}^{-3}$]	0.150 \pm 0.0 67 (0.144)	0.103 \pm 0.0 52 (0.095)	0.215 \pm 0.1 25 (0.201)	0.172 \pm 0.0 88 (0.149)	0.159 \pm 0.0 62 (0.150)	0.096 \pm 0.0 51 (0.111)	0.140 \pm 0.0 52 (0.161)	0.146 \pm 0.0 56 (0.138)
EC _{HCl} [$\mu\text{g m}^{-3}$]	0.022 \pm 0.0 08 (0.022)	0.024 \pm 0.0 12 (0.021)	0.067 \pm 0.0 52 (0.058)	0.040 \pm 0.0 15 (0.040)	0.019 \pm 0.0 04 (0.019)	0.014 \pm 0.0 07 (0.015)	0.034 \pm 0.0 18 (0.031)	0.029 \pm 0.0 18 (0.024)
TC _{HCl} [$\mu\text{g m}^{-3}$]	0.172 \pm 0.0 70 (0.165)	0.127 \pm 0.0 61 (0.115)	0.282 \pm 0.1 75 (0.250)	0.211 \pm 0.1 01 (0.175)	0.178 \pm 0.0 64 (0.169)	0.110 \pm 0.0 57 (0.128)	0.174 \pm 0.0 68 (0.194)	0.175 \pm 0.0 74 (0.162)
CC [$\mu\text{g m}^{-3}$]	0.047 \pm 0.0 28 (0.052)	0.066 \pm 0.0 68 (0.030)	0.071 \pm 0.1 31 (0.034)	0.029 \pm 0.0 51 (0.010)	0.032 \pm 0.0 36 (0.020)	0.015 \pm 0.0 18 (0.006)	0.035 \pm 0.0 48 (0.014)	0.011 \pm 0.0 11 (0.007)
TC/mas s [%]	10.3 \pm 3.8 (9.4)	6.0 \pm 1.9 (5.9)	7.8 \pm 3.5 (8.3)	5.9 \pm 2.4 (5.4)	13.2 \pm 5.4 (13.7)	8.3 \pm 6.2 (7.3)	6.0 \pm 1.6 (5.2)	7.8 \pm 1.8 (7.3)
CC/TC [%]	21.1 \pm 11.2 (19.5)	26.1 \pm 19.8 (32.7)	15.2 \pm 10.6 (13.8)	9.6 \pm 15.9 (4.3)	13.5 \pm 14.2 (6.2)	10.2 \pm 7.1 (8.9)	13.2 \pm 15.2 (8.0)	6.8 \pm 6.4 (4.4)
CC _{iso} /T C [%]	15.0 \pm 9.6 (14.9)	22.0 \pm 16.0 (15.6)	8.5 \pm 8.5 (6.7)	7.8 \pm 17.9 (1.2)	14.2 \pm 12.6 (9.8)	4.6 \pm 5.3 (4.4)	10.3 \pm 17.4 (0.2)	1.2 \pm 2.4 (0.0)
OC _{HCl} /T C [%]	68.3 \pm 12.5 (69.1)	59.0 \pm 18.1 (55.5)	65.6 \pm 9.5 (68.9)	72.5 \pm 13.9 (75.7)	76.5 \pm 12.8 (81.8)	77.7 \pm 6.3 (79.0)	71.0 \pm 13.4 (76.4)	78.5 \pm 4.6 (79.5)
EC _{HCl} /T C [%]	10.6 \pm 3.0 (10.5)	14.9 \pm 8.5 (12.7)	19.2 \pm 2.7 (20.2)	17.9 \pm 5.1 (16.5)	10.0 \pm 3.6 (9.3)	12.0 \pm 3.2 (11.6)	15.8 \pm 4.7 (15.8)	14.7 \pm 3.4 (13.3)
TC _{EA} [$\mu\text{g m}^{-3}$]	0.218 \pm 0.1 01 (0.214)	0.184 \pm 0.1 18 (0.120)	0.345 \pm 0.2 63 (0.287)	0.234 \pm 0.1 19 (0.200)	0.199 \pm 0.0 79 (0.174)	0.126 \pm 0.0 67 (0.124)	0.227 \pm 0.1 00 (0.224)	0.195 \pm 0.0 83 (0.191)
$\delta^{13}\text{C}_{\text{TC}}$ [‰]	-22.7 \pm 2.7 (-23.0)	-21.2 \pm 4.5 (-23.4)	-24.8 \pm 2.4 (-25.9)	-22.8 \pm 4.4 (-24.0)	-22.6 \pm 3.2 (-24.0)	-24.2 \pm 1.6 (-24.9)	-23.4 \pm 4.3 (-25.6)	-24.5 \pm 0.6 (-24.3)
TC _{EA-HCl} [$\mu\text{g m}^{-3}$]	0.141 \pm 0.0 63 (0.136)	0.092 \pm 0.0 52 (0.079)	0.273 \pm 0.1 96 (0.253)	0.199 \pm 0.1 08 (0.169)	0.157 \pm 0.0 65 (0.144)	0.103 \pm 0.0 52 (0.099)	0.173 \pm 0.0 68 (0.188)	0.184 \pm 0.0 80 (0.166)
$\delta^{13}\text{C}_{\text{TC-HCl}}$ [‰]	-26.6 \pm 0.7 (-26.6)	-27.0 \pm 1.1 (-27.2)	-27.1 \pm 0.9 (-27.0)	-24.4 \pm 1.1 (-24.3)	-26.2 \pm 0.5 (-26.2)	-25.3 \pm 0.8 (-25.2)	-26.0 \pm 0.4 (-26.1)	-24.7 \pm 0.8 (-24.7)
WS [m s^{-1}]	5.1 \pm 1.8 (4.5)	5.5 \pm 2.7 (5.6)	3.9 \pm 2.7 (3.1)	3.0 \pm 1.4 (3.5)	4.2 \pm 1.8 (4.6)	2.5 \pm 1.2 (2.1)	3.6 \pm 1.8 (3.4)	2.7 \pm 0.6 (2.6)
Temp. [°C]	5.0 \pm 4.6 (4.2)	-13.8 \pm 6.9 (-14.0)	-28.7 \pm 4.0 (-27.6)	-20.5 \pm 8.4 (-21.3)	1.2 \pm 4.6 (1.5)	-18.6 \pm 6.8 (-19.6)	-26.2 \pm 3.9 (-25.5)	-30.0 \pm 3.5 (-30.8)

430



431 **References:**

- 432 Arnalds, O., Dagsson-Waldhauserova, P. and Olafsson, H.: The Icelandic volcanic aeolian environment: Processes
433 and impacts - A review, *Aeolian Res.*, 20, 176–195, doi:10.1016/j.aeolia.2016.01.004, 2016.
- 434 Barrie, L. A. and Barrie, M. J.: Chemical components of lower tropospheric aerosols in the high Arctic: Six years of
435 observations, *J. Atmos. Chem.*, 11(3), 211–226, doi:10.1007/BF00118349, 1990.
- 436 Bauer, J. J., Yu, X.-Y., Cary, R., Laulainen, N. and Berkowitz, C.: Characterization of the sunset semi-continuous
437 carbon aerosol analyzer., *J. Air Waste Manag. Assoc.*, 59(7), 826–833, doi:10.3155/1047-3289.59.7.826, 2009.
- 438 Beauchamp, B., Oldershaw, A. E. and Krouse, H. R.: Upper carboniferous to upper permian ¹³C-enriched primary
439 carbonates in the sverdrup basin, Canadian arctic: Comparisons to coeval Western North American Ocean Margins,
440 *Chem. Geol. Isot. Geosci. Sect.*, 65(3–4), 391–413, doi:10.1016/0168-9622(87)90016-9, 1987.
- 441 Carslaw, K. S., Lee, L. A., Reddington, C. L., Pringle, K. J., Rap, A., Forster, P. M., Mann, G. W., Spracklen, D. V.,
442 Woodhouse, M. T., Regayre, L. A. and Pierce, J. R.: Large contribution of natural aerosols to uncertainty in indirect
443 forcing, *Nature*, 503(7474), 67–71, doi:10.1038/nature12674, 2013.
- 444 Cavalli, F., Viana, M., Yttri, K. E., Genberg, J. and Putaud, J.-P.: Toward a standardised thermal-optical protocol for
445 measuring atmospheric organic and elemental carbon: the EUSAAR protocol, *Atmos. Meas. Tech.*, 3(1), 79–89,
446 doi:10.5194/amt-3-79-2010, 2010.
- 447 Ceburnis, D., Masalaite, A., Ovadnevaite, J., Garbaras, A., Remeikis, V., Maenhaut, W., Claeys, M., Sciare, J.,
448 Baisnée, D. and O’Dowd, C. D.: Stable isotopes measurements reveal dual carbon pools contributing to organic
449 matter enrichment in marine aerosol, *Sci. Rep.*, 6(July), 1–6, doi:10.1038/srep36675, 2016.
- 450 Chave, K. E.: Carbonates: Association with organic matter in surface seawater, *Science (80-.)*, 148(June), 1723–
451 1724, doi:doi:10.1126/science.148.3678.1723, 1965.
- 452 Chave, K. E. and Suess, E.: Calcium Carbonate Saturation in Seawater: Effects of Dissolved Organic Matter,
453 *Limnol. Oceanogr.*, 15(4), 633–637, doi:10.4319/lo.1970.15.4.0633, 1970.
- 454 Chen, B., Cui, X. and Wang, Y.: Regional prediction of carbon isotopes in soil carbonates for Asian dust source
455 tracer, *Atmos. Environ.*, 142, 1–8, doi:10.1016/j.atmosenv.2016.07.029, 2016.
- 456 Chen, P., Kang, S., Abdullaev, S. F., Safarov, M. S., Huang, J., Hu, Z., Tripathee, L. and Li, C.: Significant
457 influence of carbonates on determining organic carbon and black carbon: A case study in Tajikistan, central Asia,
458 *Environ. Sci. Technol.*, 55(5), 2839–2846, doi:10.1021/acs.est.0c05876, 2021.
- 459 Chow, J. C., Watson, J. G., Pritchett, L. C., Pierson, W. R., Frazier, C. A. and Purcell, R. G.: The dri thermal/optical
460 reflectance carbon analysis system: description, evaluation and applications in U.S. Air quality studies, *Atmos.*
461 *Environ.*, 27A(8), 1185–1201, 1993.



- 462 Chow, J. C., Watson, J. G., Chen, L.-W. A., Chang, M. C. O., Robinson, N. F., Trimble, D. and Kohl, S.: The
463 IMPROVE_A temperature protocol for thermal/optical carbon analysis: maintaining consistency with a long-term
464 database., *J. Air Waste Manage. Assoc.*, 57(9), 1014–1023, doi:10.3155/1047-3289.57.9.1014, 2007.
- 465 Descolas-Gros, C. and Fontugne, M.: Stable carbon isotope fractionation by marine phytoplankton during
466 photosynthesis, *Plant. Cell Environ.*, 13(3), 207–218, doi:10.1111/j.1365-3040.1990.tb01305.x, 1990.
- 467 England, M. R., Eisenman, I., Lutsko, N. J. and Wagner, T. J. W.: The Recent Emergence of Arctic Amplification,
468 *Geophys. Res. Lett.*, 48(15), 1–10, doi:10.1029/2021GL094086, 2021.
- 469 Feltracco, M., Barbaro, E., Spolaor, A., Vecchiato, M., Callegaro, A., Burgay, F., Vardè, M., Maffezzoli, N., Dallo,
470 F., Scoto, F., Zangrando, R., Barbante, C. and Gambaro, A.: Year-round measurements of size-segregated low
471 molecular weight organic acids in Arctic aerosol, *Sci. Total Environ.*, 763, 142954,
472 doi:10.1016/j.scitotenv.2020.142954, 2021.
- 473 Flanner, M. G., Zender, C. S., Randerson, J. T. and Rasch, P. J.: Present-day climate forcing and response from
474 black carbon in snow, *J. Geophys. Res.*, 112(D11), D11202, doi:10.1029/2006JD008003, 2007.
- 475 Friman, M., Aurela, M., Saarnio, K., Teinilä, K., Kesti, J., Harni, S. D., Saarikoski, S., Hyvärinen, A. and Timonen,
476 H.: Long-term characterization of organic and elemental carbon at three different background areas in northern
477 Europe, *Atmos. Environ.*, 310(February), doi:10.1016/j.atmosenv.2023.119953, 2023.
- 478 Gensch, I., Kiendler-Scharr, A. and Rudolph, J.: Isotope ratio studies of atmospheric organic compounds: Principles,
479 methods, applications and potential, *Int. J. Mass Spectrom.*, 365–366, 206–221, doi:10.1016/j.ijms.2014.02.004,
480 2014.
- 481 Groot Zwaaftink, C. D., Grythe, H., Skov, H. and Stohl, A.: Substantial contribution of northern high-latitude
482 sources to mineral dust in the Arctic, *J. Geophys. Res.*, 121(22), 13,678–13,697, doi:10.1002/2016JD025482, 2016.
- 483 Gu, W., Xie, Z., Wei, Z., Chen, A., Jiang, B., Yue, F. and Yu, X.: Marine Fresh Carbon Pool Dominates Summer
484 Carbonaceous Aerosols Over Arctic Ocean, *J. Geophys. Res. Atmos.*, 128(8), doi:10.1029/2022JD037692, 2023.
- 485 Hasegawa, S.: Experimental Characterization of PM_{2.5} Organic Carbon by Using Carbon-fraction Profiles of
486 Organic Materials, *Asian J. Atmos. Environ.*, 16(2), 2021128, doi:10.5572/ajae.2021.128, 2022.
- 487 Holtz, L. M., Wolf-Gladrow, D. and Thoms, S.: Stable carbon isotope signals in particulate organic and inorganic
488 carbon of coccolithophores – A numerical model study for *Emiliania huxleyi*, *J. Theor. Biol.*, 420(January), 117–
489 127, doi:10.1016/j.jtbi.2017.01.030, 2017.
- 490 Hu, Z., Kang, S., Xu, J., Zhang, C., Li, X., Yan, F., Zhang, Y., Chen, P. and Li, C.: Significant overestimation of
491 black carbon concentration caused by high organic carbon in aerosols of the Tibetan Plateau, *Atmos. Environ.*,
492 294(June 2022), 119486, doi:10.1016/j.atmosenv.2022.119486, 2023.
- 493 Huang, L., Brook, J. R., Zhang, W., Li, S. M., Graham, L., Ernst, D., Chivulescu, A. and Lu, G.: Stable isotope



- 494 measurements of carbon fractions (OC/EC) in airborne particulate: A new dimension for source characterization and
495 apportionment, *Atmos. Environ.*, 40(15), 2690–2705, doi:10.1016/j.atmosenv.2005.11.062, 2006.
- 496 Huang, L., Zhang, W., Santos, G. M., Rodríguez, B. T., Holden, S. R., Vetro, V. and Czimeczik, C. I.: Application of
497 the ECT9 protocol for radiocarbon-based source apportionment of carbonaceous aerosols, *Atmos. Meas. Tech.*,
498 14(5), 3481–3500, doi:10.5194/amt-14-3481-2021, 2021.
- 499 Kawai, K., Matsui, H. and Tobo, Y.: Dominant Role of Arctic Dust With High Ice Nucleating Ability in the Arctic
500 Lower Troposphere, *Geophys. Res. Lett.*, 50(8), 1–10, doi:10.1029/2022GL102470, 2023.
- 501 Kawamura, K. and Watanabe, T.: Determination of stable carbon isotopic compositions of low molecular weight
502 dicarboxylic acids and ketocarboxylic acids in atmospheric aerosol and snow samples, *Anal. Chem.*, 76(19), 5762–
503 5768, doi:10.1021/ac049491m, 2004.
- 504 Kawamura, K., Yanase, A., Eguchi, T., Mikami, T. and Barrie, L. A.: Enhanced atmospheric transport of soil
505 derived organic matter in spring over the Arctic, *Geophys. Res. Lett.*, 23(25), 3735–3738, doi:10.1029/96GL03537,
506 1996.
- 507 Laskin, A., Laskin, J. and Nizkorodov, S. a.: Chemistry of Atmospheric Brown Carbon, *Chem. Rev.*, 115(10), 4335–
508 4382, doi:10.1021/cr5006167, 2015.
- 509 Liu, D., He, C., Schwarz, J. P. and Wang, X.: Lifecycle of light-absorbing carbonaceous aerosols in the atmosphere,
510 *npj Clim. Atmos. Sci.*, 3(1), doi:10.1038/s41612-020-00145-8, 2020.
- 511 Mbengue, S., Zikova, N., Schwarz, J., Vodička, P., Šmejkalová, A. H. and Holoubek, I.: Mass absorption cross-
512 section and absorption enhancement from long term black and elemental carbon measurements: A rural background
513 station in Central Europe, *Sci. Total Environ.*, 794, doi:10.1016/j.scitotenv.2021.148365, 2021.
- 514 McClelland, H. L. O., Bruggeman, J., Hermoso, M. and Rickaby, R. E. M.: The origin of carbon isotope vital effects
515 in coccolith calcite, *Nat. Commun.*, 8(May 2016), 1–16, doi:10.1038/ncomms14511, 2017.
- 516 Meinander, O., Dagsson-Waldhauserova, P., Amosov, P., Aseyeva, E., Atkins, C., Baklanov, A., Baldo, C., Barr, S.
517 L., Barzycka, B., Benning, L. G., Cvetkovic, B., Enchilik, P., Frolov, D., Gassó, S., Kandler, K., Kasimov, N.,
518 Kavan, J., King, J., Koroleva, T., Krupskaya, V., Kulmala, M., Kusiak, M., Lappalainen, H. K., Laska, M., Lasne, J.,
519 Lewandowski, M., Luks, B., Mcquaid, J. B., Moroni, B., Murray, B., Möhler, O., Nawrot, A., Nickovic, S., O’neill,
520 N. T., Pejanovic, G., Popovicheva, O., Ranjbar, K., Romanias, M., Samonova, O., Sanchez-Marroquin, A.,
521 Schepanski, K., Semenkov, I., Sharapova, A., Shevnina, E., Shi, Z., Sofiev, M., Thevenet, F., Thorsteinsson, T.,
522 Timofeev, M., Umo, N. S., Uppstu, A., Urupina, D., Varga, G., Werner, T., Arnalds, O. and Vukovic Vicmic, A.:
523 Newly identified climatically and environmentally significant high-latitude dust sources, *Atmos. Chem. Phys.*,
524 22(17), 11889–11930, doi:10.5194/acp-22-11889-2022, 2022.
- 525 Monteiro, F. M., Bach, L. T., Brownlee, C., Bown, P., Rickaby, R. E. M., Poulton, A. J., Tyrrell, T., Beaufort, L.,
526 Dutkiewicz, S., Gibbs, S., Gutowska, M. A., Lee, R., Riebesell, U., Young, J. and Ridgwell, A.: Why marine



- 527 phytoplankton calcify, *Sci. Adv.*, 2(7), 1–14, doi:10.1126/sciadv.1501822, 2016.
- 528 Moschos, V., Dzepina, K., Bhattu, D., Lamkaddam, H., Casotto, R., Daellenbach, K. R., Canonaco, F., Rai, P., Aas,
529 W., Becagli, S., Calzolari, G., Eleftheriadis, K., Moffett, C. E., Schnelle-Kreis, J., Severi, M., Sharma, S., Skov, H.,
530 Vestenius, M., Zhang, W., Hakola, H., Hellén, H., Huang, L., Jaffrezo, J. L., Massling, A., Nøjgaard, J. K., Petäjä,
531 T., Popovicheva, O., Sheesley, R. J., Traversi, R., Yttri, K. E., Schmale, J., Prévôt, A. S. H., Baltensperger, U. and
532 El Haddad, I.: Equal abundance of summertime natural and wintertime anthropogenic Arctic organic aerosols, *Nat.*
533 *Geosci.*, doi:10.1038/s41561-021-00891-1, 2022.
- 534 Muller, A., Lamb, E. G. and Siciliano, S. D.: The silent carbon pool: Cryoturbic enriched organic matter in Canadian
535 High Arctic semi-deserts, *Geoderma*, 415(September 2021), 115781, doi:10.1016/j.geoderma.2022.115781, 2022.
- 536 Narukawa, M., Kawamura, K., Li, S.-M. and Bottenheim, J. W.: Stable carbon isotopic ratios and ionic composition
537 of the high-Arctic aerosols: An increase in $\delta^{13}\text{C}$ values from winter to spring, *J. Geophys. Res.*, 113(D2), D02312,
538 doi:10.1029/2007JD008755, 2008.
- 539 Not, C. and Hillaire-Marcel, C.: Enhanced sea-ice export from the Arctic during the Younger Dryas, *Nat. Commun.*,
540 3(April 2014), 645–647, doi:10.1038/ncomms1658, 2012.
- 541 Okada, H. and Honjo, S.: Distribution of Oceanic Coccolithophorids in the Pacific., *Deep Sea Res.*, 20(4), 355–374,
542 doi:10.1016/0011-7471(73)90059-4, 1973.
- 543 Petit, J. E., Favez, O., Albinet, A. and Canonaco, F.: A user-friendly tool for comprehensive evaluation of the
544 geographical origins of atmospheric pollution: Wind and trajectory analyses, *Environ. Model. Softw.*, 88, 183–187,
545 doi:10.1016/j.envsoft.2016.11.022, 2017.
- 546 Petzold, A., Ogren, J. A., Fiebig, M., Laj, P., Li, S. M., Baltensperger, U., Holzer-Popp, T., Kinne, S., Pappalardo,
547 G., Sugimoto, N., Wehrli, C., Wiedensohler, A. and Zhang, X. Y.: Recommendations for reporting black carbon
548 measurements, *Atmos. Chem. Phys.*, 13(16), 8365–8379, doi:10.5194/acp-13-8365-2013, 2013.
- 549 Phillips, R. L. and Grantz, A.: Regional variations in provenance and abundance of ice-rafted clasts in Arctic Ocean
550 sediments: Implications for the configuration of late Quaternary oceanic and atmospheric circulation in the Arctic,
551 *Mar. Geol.*, 172(1–2), 91–115, doi:10.1016/S0025-3227(00)00101-8, 2001.
- 552 Pushkareva, E., Johansen, J. R. and Elster, J.: A review of the ecology, ecophysiology and biodiversity of
553 microalgae in Arctic soil crusts, *Polar Biol.*, 39(12), 2227–2240, doi:10.1007/s00300-016-1902-5, 2016.
- 554 Rodríguez, B. T., Huang, L., Santos, G. M., Zhang, W., Vetro, V., Xu, X., Kim, S. and Czimeczik, C. I.: Seasonal
555 Cycle of Isotope-Based Source Apportionment of Elemental Carbon in Airborne Particulate Matter and Snow at
556 Alert, Canada, *J. Geophys. Res. Atmos.*, 125(23), 1–15, doi:10.1029/2020JD033125, 2020.
- 557 Savadkoobi, M., Pandolfi, M., Favez, O., Putaud, J. P., Eleftheriadis, K., Fiebig, M., Hopke, P. K., Laj, P.,
558 Wiedensohler, A., Alados-Arboledas, L., Bastian, S., Chazeanu, B., María, Á. C., Colombi, C., Costabile, F., Green,



- 559 D. C., Hueglin, C., Liakakou, E., Luoma, K., Listrani, S., Mihalopoulos, N., Marchand, N., Močnik, G., Niemi, J.
560 V., Ondráček, J., Petit, J. E., Rattigan, O. V., Reche, C., Timonen, H., Titos, G., Tremper, A. H., Vratolis, S.,
561 Vodička, P., Funes, E. Y., Zíková, N., Harrison, R. M., Petäjä, T., Alastuey, A. and Querol, X.: Recommendations
562 for reporting equivalent black carbon (eBC) mass concentrations based on long-term pan-European in-situ
563 observations, *Environ. Int.*, 185(December 2023), 108553, doi:10.1016/j.envint.2024.108553, 2024.
- 564 Sharma, S., Lavoué, D., Chachier, H., Barrie, L. A. and Gong, S. L.: Long-term trends of the black carbon
565 concentrations in the Canadian Arctic, *J. Geophys. Res. D Atmos.*, 109(15), 1–10, doi:10.1029/2003JD004331,
566 2004.
- 567 Sharma, S., Leaitch, W. R., Huang, L., Veber, D., Kolonjari, F., Zhang, W., Hanna, S. J., Bertram, A. K. and Ogren,
568 J. A.: An evaluation of three methods for measuring black carbon in Alert, Canada, *Atmos. Chem. Phys.*, 17(24),
569 15225–15243, doi:10.5194/acp-17-15225-2017, 2017.
- 570 Sharma, S., Barrie, L. A., Magnusson, E., Brattström, G., Leaitch, W. R., Steffen, A. and Landsberger, S.: A Factor
571 and Trends Analysis of Multidecadal Lower Tropospheric Observations of Arctic Aerosol Composition, Black
572 Carbon, Ozone, and Mercury at Alert, Canada, *J. Geophys. Res. Atmos.*, 124(24), 14133–14161,
573 doi:10.1029/2019JD030844, 2019.
- 574 Sirois, A. and Barrie, L. A.: Arctic lower tropospheric aerosol trends and composition at Alert, Canada: 1980-1995,
575 *J. Geophys. Res.*, 104(D9), 11599–11618, 1999.
- 576 Smith, H. E. K., Tyrrell, T., Charalampopoulou, A., Dumousseaud, C., Legge, O. J., Birchenough, S., Pettit, L. R.,
577 Garley, R., Hartman, S. E., Hartman, M. C., Sagoo, N., Daniels, C. J., Achterberg, E. P. and Hydes, D. J.:
578 Predominance of heavily calcified coccolithophores at low CaCO₃ saturation during winter in the Bay of Biscay,
579 *Proc. Natl. Acad. Sci. U. S. A.*, 109(23), 8845–8849, doi:10.1073/pnas.1117508109, 2012.
- 580 Stein, A. F., Draxler, R. R., Rolph, G. D., Stunder, B. J. B., Cohen, M. D. and Ngan, F.: NOAA's HYSPLIT
581 atmospheric transport and dispersion modeling system, *Bull. Am. Meteorol. Soc.*, 96(12), 2059–2077,
582 doi:10.1175/BAMS-D-14-00110.1, 2015.
- 583 Stein, R., Grobe, H. and Wahsner, M.: Organic carbon, carbonate, and clay mineral distributions in eastern central
584 Arctic Ocean surface sediments, *Mar. Geol.*, 119(3–4), 269–285, doi:10.1016/0025-3227(94)90185-6, 1994.
- 585 Stjern, C. W., Samset, B. H., Myhre, G., Bian, H., Chin, M., Davila, Y., Dentener, F., Emmons, L., Flemming, J.,
586 Haslerud, A. S., Henze, D., Jonson, J. E., Kucsera, T., Lund, M. T., Schulz, M., Sudo, K., Takemura, T. and Tilmes,
587 S.: Global and regional radiative forcing from 20 % reductions in BC, OC and SO₄ - An HTAP2 multi-model study,
588 *Atmos. Chem. Phys.*, 16(21), 13579–13599, doi:10.5194/acp-16-13579-2016, 2016.
- 589 Toom-Sauntry, D. and Barrie, L. A.: Chemical composition of snowfall in the high Arctic: 1990-1994, *Atmos.*
590 *Environ.*, 36(15–16), 2683–2693, doi:10.1016/S1352-2310(02)00115-2, 2002.
- 591 Verwega, M. T., Somes, C. J., Schartau, M., Tuerena, R. E., Lorrain, A., Oschlies, A. and Slawig, T.: Description of



- 592 a global marine particulate organic carbon-13 isotope data set, *Earth Syst. Sci. Data*, 13(10), 4861–4880,
593 doi:10.5194/essd-13-4861-2021, 2021.
- 594 Vodička, P., Kawamura, K., Schwarz, J. and Ždímal, V.: Seasonal changes in stable carbon isotopic composition in
595 the bulk aerosol and gas phases at a suburban site in Prague, *Sci. Total Environ.*, 803, 149767,
596 doi:10.1016/j.scitotenv.2021.149767, 2022.
- 597 Wang, H. and Kawamura, K.: Stable carbon isotopic composition of low-molecular-weight dicarboxylic acids and
598 ketoacids in remote marine aerosols, *J. Geophys. Res. Atmos.*, 111(7), doi:10.1029/2005JD006466, 2006.
- 599 Winiger, P., Barrett, T. E., Sheesley, R. J., Huang, L., Sharma, S., Barrie, L. A., Yttri, K. E., Evangeliou, N.,
600 Eckhardt, S., Stohl, A., Klimont, Z., Heyes, C., Semiletov, I. P., Dudarev, O. V., Charkin, A., Shakhova, N.,
601 Holmstrand, H., Andersson, A. and Gustafsson: Source apportionment of circum-Arctic atmospheric black carbon
602 from isotopes and modeling, *Sci. Adv.*, 5(2), 1–10, doi:10.1126/sciadv.aau8052, 2019.
- 603 Zeebe, R. E.: History of seawater carbonate chemistry, atmospheric CO₂, and ocean acidification, *Annu. Rev. Earth
604 Planet. Sci.*, 40, 141–165, doi:10.1146/annurev-earth-042711-105521, 2012.
- 605